3 Biotech (2023) 13:337
https://doi.org/10.1007/s13205-023-03725-6

ORIGINAL ARTICLE

In vitro and in silico cholinesterase inhibitory potential of metabolites from *Laurencia snackeyi* (Weber-van Bosse) M. Masuda

Kishneth Palaniveloo[1,2] · Kuan Hung Ong[1] · Herland Satriawan[1] · Shariza Abdul Razak[3] · Suciati Suciati[4] · Hsin-Yi Hung[5] · Shin Hirayama[6] · Mohammed Rizman-Idid[1] · Jen Kit Tan[7] · Yoong Soon Yong[8] · Siew-Moi Phang[1,8]

Received: 2 June 2023 / Accepted: 1 August 2023 / Published online: 10 September 2023
© King Abdulaziz City for Science and Technology 2023

Abstract

Alzheimer's disease (AD) is a neurodegenerative disease that causes deterioration in intelligence and psychological activities. Yet, till today, no cure is available for AD. The marine environment is an important sink of bioactive compounds with neuroprotective potential with reduced adverse effects. Recently, we collected the red algae *Laurencia snackeyi* from Terumbu Island, Malaysia which is known to be rich in halogenated metabolites making it the most sought-after red algae for pharmaceutical studies. The red alga was identified based on basic morphological characteristics, microscopic observation and chemical data from literature. The purplish-brown algae was confirmed a new record. In Malaysia, this species is poorly documented in Peninsular Malaysia as compared to its eastern continent Borneo. Thus, this study intended to investigate the diversity of secondary metabolites present in the alga and its cholinesterase inhibiting potential for AD. The extract inhibited both acetylcholinesterase (AChE) and butyrylcholinesterase (BChE) with IC_{50} values of 14.45 ± 0.34 µg mL^{-1} and 39.59 ± 0.24 µg mL^{-1}, respectively. Subsequently, we isolated the synderanes, palisadin A (**1**), aplysistatin (**2**) and 5-acetoxypalisadin B (**3**) that was not exhibit potential. Mass spectrometry analysis detected at total of 33 additional metabolites. The computational aided molecular docking using the AChE and BChE receptors on all metabolites shortlisted 5,8,11,14-eicosatetraynoic acid (**31**) and 15-hydroxy-1-[2-(hydroxymethyl)-1-piperidinyl]prost-13-ene-1,9-dione (**42**) with best inhibitory properties, respectively with the lowest optimal combination of S-score and RMSD values. This study shows the unexplored potential of marine natural resources, however, obtaining sufficient biomass for detailed investigation is an uphill task. Regardless, there is a lot of potential for future prospects with a wide range of marine natural resources to study and the incorporation of synthetic chemistry, in vivo studies in experimental design.

Keywords Chemotaxonomy · Neurodegenerative · Rhodophyta · Secondary metabolites · Alzheimer's · *Laurencia snackeyi*

Introduction

Alzheimer's disease (AD) is a chronic neurodegenerative disorder that causes deterioration in intelligence and psychological activities. First described in 1906, it is considered among the highest causes of death from a neurodegenerative disease globally estimated at approximately 60–70% cases. Globally, the number of AD patients is expected to rise three folds from 46.8 million by 2050 due to increase in financial and social burden (Ferreira et al. 2021). Often associated to aging, among early signs of AD are short-term memory loss, communication problems, disorientation, loss of motivation, neglect in self-care, sleep disorders and behavioral issues (Ferreira et al. 2021). With time, chronic symptoms are loss of thinking capability, behavioral disturbances, neuronal death, memory loss, cognitive deficit, and cholinergic dysfunction that are associated to the loss of neurotransmitter acetylcholine (ACh) from the neurons in the central nervous system (Srivastava et al. 2019) Apart from genetic and environment, the cholinesterase (acetyl- and butyrylcholinesterase) enzymes, β-amyloid (Aβ) aggregation, protein kinase C, tau protein, proteases with β-site amyloid precursor protein cleaving cascade (β- and γ-secretases), glycogen-synthase kinase 3β (GSK-3β), neurodegenerators, and oxidants are

Kishneth Palaniveloo, Kuan Hung Ong, Herland Satriawan, Shariza Abdul Razak, Suciati Suciati, Hung Hsin-Yi, Shin Hirayama, Mohammed Rizman-Idid, Jen Kit Tan, Yoong Soon Yong, and Siew-Moi Phang have contributed equally to this work.

Extended author information available on the last page of the article

recognized as factors for AD (Ghoran et al. 2021). To date, there are no available drugs to stop or alter AD progression, instead only improve its symptoms for a limited time for fortunate patients (Tripathi et al. 2019). Among the common restrictions of readily available drugs (eg. rivastigmine, galantamine and donepezil) for AD are toxicity, short half-life, allergic reactions and high cost (Kabir et al. 2021). In search for pharmacologically active metabolites, much attention is given to the marine environment that is an important sink of structurally diverse chemical groups such as polysaccharides, carotenoids, polyphenols, sterol and alkaloids. Marine derived metabolites have exhibited neuroprotective activities with reduced adverse events (Kabir et al. 2021; Hu et al. 2023). Nowadays, the use of chemo-informatics study and computer-aided drug design (CADD) are the way forward in drug discovery, design, and development. Fast, inexpensive techniques to examine binding interactions, inspect pharmacokinetic houses and bioactivity parameters in search for novel inhibitors with higher biochemical interactions such as the use of molecular docking analysis, pharmacokinetics study and bioactivity predictions are making the search for potent drugs more accessible (Abduljelil et al. 2022). The red algae genus *Laurencia* is one of the richest marine source of secondary metabolites. Currently there are a total of 146 accepted species taxonomically and is widely distributed in tropical waters. Often associated to degraded parts of the reefs, the chemical diversity of *Laurencia* had been studied for more than half a decade. It is well established that several species possess unique chemical signatures, for instance, *L. snackeyi* (Weber-van Bosse) M. Masuda (1997) is considered a producer of synderane type metabolites, *L. majuscula* is known for its charmigrane type sesquiterpenes, *L. similis* synthesizes bromoindoles and aristolane while *L. nangii* is well documented for the production of C_{15} acetogenins (Palaniveloo and Vairappan 2014; Vairappan et al. 2004; Kamada and Vairappan 2012). In a recent Marine Park dive expedition funded by the Department of Fisheries Malaysia, we collected *L. snackeyi* specimen at Pulau Terumbu off Port Dickson. This manuscript confirms this finding as a first record from this island and second from Peninsular Malaysia. The only known report was from Pulau Besar, Malacca in 1997 Masuda et al. (1997). This manuscript elaborates the chemical diversity in the *L. snackeyi* extract via chromatographic isolation and mass spectrometry analysis. The seaweed extract was evaluated for its in vitro potential as an anti-Alzheimer's agent based on its acetylcholinesterase (AChE) and butyrylcholinesterase (BChE) enzyme inhibitory activity followed by a molecular docking analysis of all metabolites identified from the extract.

Materials and methods

Sampling site and plant material

Laurencia snackeyi specimens were collected from Terumbu Island, Port Dickson, Negeri Sembilan (02.463456 °N, 101.845939 °E) during the Biodiversity Expedition in Malacca and Negeri Sembilan 2018. Plant materials were collected via SCUBA at the depths of 3–5 m, immediately cleaned-off from foreign matters, rinsed in clean seawater, and kept under cool (< 20 °C) conditions. Underwater, the red alga was recognised by its thick main axes arising from a discoid holdfast and without stolon-like branches. Upright thalli are greenish purple to brownish. Its physical texture is firm and fleshy. The voucher specimen (PSM13824) was prepared and kept in IOES, Universiti Malaya.

Chemical extraction

The partially dried algae (47 g) was extracted in 500 mL of analytical grade methanol (MeOH) (Merck, Germany), concentrated in vacuo and repeatedly partitioned between analytical grade ethyl acetate (EtOAc) (Merck, Germany) and distilled water (H_2O) at a ratio of 1:3. The EtOAc solution was dried over anhydrous sodium sulphate (Na_2SO_4) (Sigma-Aldrich, USA), and evaporated to obtain a dark green paste (200 mg).

Cholinesterase inhibitory activity

Cholinesterase inhibition assays

This assay was carried out according to the modified Ellman's method (Ellman et al. 1961; Aristyawan et al. 2022; Chang et al. 2023; Zhan et al. 2023). The *Laurencia* extract was dissolved in methanol to a final concentration of 1 mg mL^{-1} and serially diluted (0.01–300 µg mL^{-1}). Sample solutions (25 µL) were added to a 96-well microplate, followed by 25 µL of 1.5 mM acetylthiocholine iodide (ATCI, Sigma-Aldrich, USA) as a substrate for the AChE enzyme from electric eel type VI-S, and 25 µL of butyrylthiocholine iodide (BTCI, Sigma-Aldrich, USA) as a substrate for the BChE enzyme from equine serum. Then 125 µL of 3 mM Ellman's reagent (DTNB, Sigma-Aldrich, USA), Tris-buffer (50 µL), and AChE or BChE enzymes (25 µL) 0.22 U mL^{-1} was added to hydrolyze the substrate. Before measurement, the solutions were shaken for 30 s in a microplate reader

(Thermo Scientific Multiskan FC). The yellow color from the product, 5-thio-2-nitrobenzoate, was measured at 405 nm every 5 s for 2 min. Every experiment was carried out in triplicates. Methanol 10% was used as a control. The enzyme activity was calculated as a percentage of the velocity of the sample compared with the negative control. The inhibitory activity was calculated based on Eq. 1.

$$Inhibition(\%) = ((V_{control} - V_{sample})/V_{control}) \times 100, \quad (1)$$

where V is the mean velocity

Compound isolation and characterization

Laurencia snackeyi extract was subjected to high performance liquid chromatography (HPLC) profiling on a HPLC system (Nexera; Shimadzu, Japan) configured with a pump (LC-40XR), oven (CTO-40S), and a PDA detector (SPD-M40), using a Phenomenex C18(2) column (10 × 250 mm, 5 µm) under gradient mode of MeOH-H_2O (MeOH: 50%, 0–5 min; 70%, 10–15 min; 90%, 20–25 min; 100%, 28–30 min), screened between 190 and 800 nm over a flow rate of 2 mL min^{-1}. Isolated pure compounds were subjected to ^{1}H-NMR and ^{13}C-NMR experiment on a BRUKER 600 MHz and its corresponding chemical data was compared to literature to confirm identity of isolated metabolites.

Tandem mass spectrometry (MS/MS) analysis

High resolution MS/MS analysis was performed using an Orbitrap mass spectrometry (MS) system (Thermo Fisher Scientific, Waltham, MA, USA). Sample was pre-separated using the Dionex UltiMate 3000 UHPLC system with a Syncronis C18 column (2.1 mm × 100 mm × 1.7 µm) before being directed to the MS and analysed under conditions as described in Maran et al. (2021). Acquired data was processed and analysed using the Thermo Scientific Compound Discoverer 3.3 SP1 software with the default settings (Maran et al. 2021). Identification of compound was based on the matching of MS/MS data against mzCloud database. Unmatched signals were attempted with the built-in ChemSpider workflow using accurate mass against Chemical Entities of Biological Interest (ChEBI) (Hastings et al. 2016), ChEMBL (Davies et al. 2015; Mendez et al. 2019), LIPID MAPS® Structure Database (LMSD) (Sud et al. 2006), National Institute of Standards and Technology (NIST) and PubMed databases. Matching tolerance was limited to 2 ppm mass error and minimum FISh scoring of 50.

Molecular docking

Preparation of receptor proteins and ligands

The two receptor proteins targeted for neurotransmitter choline inhibition selected for modelling were: (1) crystal structure of recombinant human acetylcholinesterase (AChE, 4EY6) with galantamine as reference ligand; (2) human butyrylcholinesterase (BChE, 4BDS) with tacrine as reference ligand (Cheung et al. 2012; Nachon et al. 2013). Suitable updated receptors were obtained from the RCSB PDB website (https://www.rcsb.org/). The binding sites were determined through literature report and predicted using the "Site Finder" algorithm in Molecular Operation Environment (MOE) 2015 software (Chemical Computing Group Inc, 2015), followed by validation with PDBsum (http://www.ebi.ac.uk/pdbsum) for the ligand-protein interactions. The receptor proteins were prepared using MOE 2015 QuickPrep module whereby energy convergence set at Root Mean Square (RMS) gradient of 0.01 kcal/mol/A^2. The receptors were prepared using Protonate3D, which was set to default to predict the hydrogen coordinates of 3D structures automatically.

For the molecular docking simulation, 33 compounds (**1–3**, **27–56**) identified from *L.snackeyi* (Figs. 4, 4, 6 and 9) were analysed. All compounds and reference structural data file (.sdf) were obtained from PubChem (https://pubchem.ncbi.nlm.nih.gov/) and drawn by ChemDraw software. A compound database was created and prepared using MOE 2015 software. The compounds were washed with the default format of MOE 2015 software to eliminate unnecessary atoms and explicit hydrogens were added. The partial charge of the compounds was subjected to MMFF94x, changed into gas phase, hydrogen and lone pair electrons were adjusted. The RMS gradient in energy minimization was set at 0.01 kcal/mol/A^2.

After the binding sites were selected and validated by literature reports and PDBsum, they were then viewed by PyMOL Educational 1.3 software (Copyright 2010 Schrodinger, LLC) to confirm the binding cleft of the receptor. The binding site for AChE are Trp86, Gly120, Gly121, Gly122, Glu202, Phe295, Phe297, Tyr337, and His447; while for BChE are Trp82, Glu197, Ala328, Tyr332, Trp430, and His438, both in Chain A of the receptor. The receptor proteins and ligands were docked by using the induced fit method with 100-1 poses (docked 100 times with one best-docked conformation being generated) using the MOE 2015 software.

Docking conformational analysis

The docking results were analyzed for their free binding energy (S-score) and root mean square deviation (RMSD). The S-score is a summary score of all interactions and bonds (e.g., hydrogen bond, van der Waals, electrostatic, solvation, etc). Low S-score indicates a stronger binding affinity between the ligand and protein receptor (Khelfaoui et al. 2021). The RMSD is a comparison between the docked conformation with the reference or with other docked conformation. RMSD with < 2Å is considered an accurate prediction of ligand binding model. The docked conformations 2D diagrams were further visualized and analyzed for their binding interactions using the Discovery Studio 2016 Client software.

Results

Morphological observation

The greenish purple seaweed found growing on coral rubble at depths of 3-5 meters of Terumbu Island (02.463456 °N, 101.845939 °E) where high surge and currents were present was identified as *L. snackeyi*. One to 6 upright thalli (Fig. 1) appeared from a discoid holdfast and without stolon-like branches. The thalli are greenish purple, firmly fleshy in the living state, and adheres to paper when dried. All characteristics fit the description of *L. snackeyi*. The light microscope image and morphology of specimen was comparable to report by Masuda et al. (1997). Voucher specimen (PSM13824) was prepared and deposited at the IOES herbarium collection at Universiti Malaya.

Fig. 1 Dissecting microscope image of *Laurencia snackeyi* (left) as compared to the microscope image as obtained by Masuda et al. (1997) (right)

Cholinesterase inhibitory potential

The methanol extracted alga (47 g, DW) yielded 200 mg (0.42%) dark-green paste. The *L. snackeyi* extracts was evaluated in vitro for its inhibition potency towards AChE and BChE through the modified Ellman's method, using galantamine as a positive control at 100 µg mL^{-1} concentration. The extract demonstrated a higher inhibition against AChE with IC_{50} value of 14.45 ± 0.34 µg mL^{-1} compared to BChE with IC_{50} value of 39.59 ± 0.24 µg mL^{-1}. The dose-response curve for *L. snackeyi* extract against AChE and BChE is shown in Fig. 2. Following this data, we decided to investigate the probable source of cholinesterase inhibitory potential from the list of metabolites identified in the extract with the assistance of molecular docking analysis.

Chemical profiling and isolation

The extract (20 mg) was chemically visualised using TLC and analysed using HPLC. A total of six (6) isolates (P1–P6) detected at retention times (RTs) 10.7, 13.9, 15.6, 16.8, 17.3 and 17.7 min, when scanned between UV wavelength 190 and 254 nm were collected and characterized using NMR. From a total of 20 mg extract, between 3 and 4 mg of biomass was obtained from isolates P1, P2 and P5 while P3, P4 and P6 yielded less than 2 mg. Figure 3 shows the HPLC chromatogram as well as the 2D and 3D PDA output for the profiled extract. The ^{1}H-NMR and ^{13}C-NMR data for three

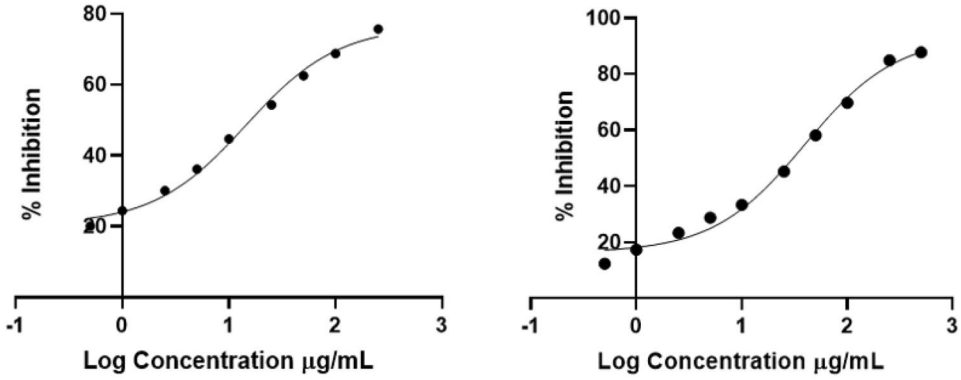

Fig. 2 Dose-response curve for *L. snackeyi* extract against AChE (left, IC_{50} = 14.45 ± 0.34 µg mL^{-1}) and BChE (right, IC_{50} = 39.59 ± 0.24 µg mL^{-1})

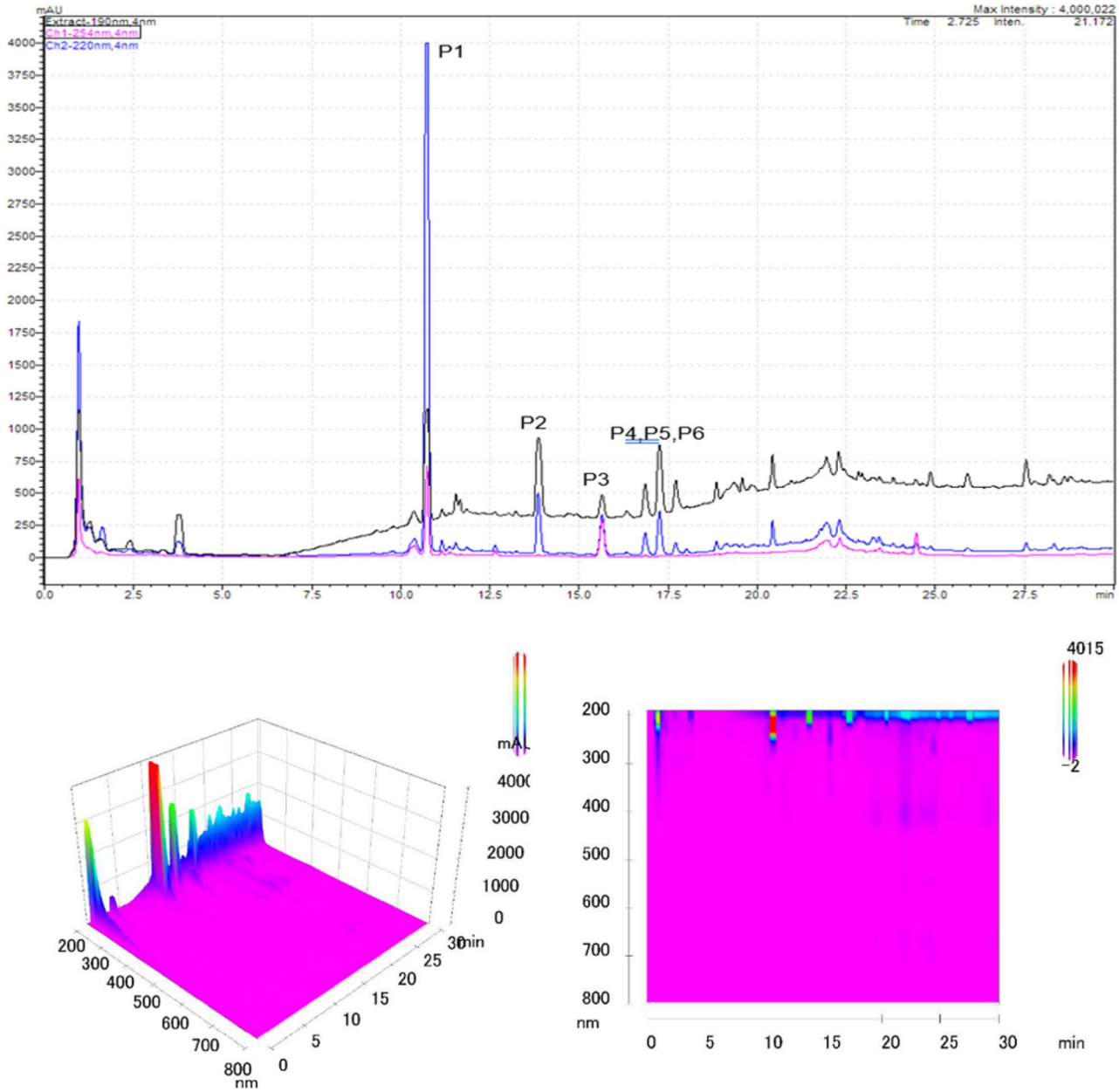

Fig. 3 Top—HPLC chromatogram of *L. snackeyi* crude extract; black (190 nm), blue (220 nm), pink (254 nm). Bottom—corresponding PDA output in 2D and 3D

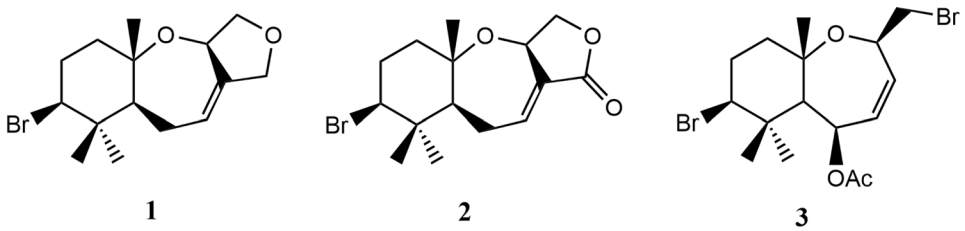

Fig. 4 Structures of the syndreans palisadin A (**1**), aplysistatin (**2**) and 5-acetoxyp-alisadin B (**3**) that was isolated from *L. snackeyi extract*

of the six (6) isolates; P1, P2 and P5, matched literature for palisadin A (**1**), aplysistatin (**2**) and 5-acetoxypalisadin B (**3**). This finding is also identical to the report by Masuda from Pulau Besar in 1997. The chemical structure for the three compounds are shown in Fig. 4 and the data for the compounds are provided below;

Palisadin A (**1**)—oil; $C_{15}H_{23}O_2Br$; ^{1}H-NMR ($CDCl_3$, 600 MHz) δ 1.16 (3H, s, H-15), 0.92 (3H, s, H3-14), 1.26 (3H, s, H-13), 4.36 (1H, dd, J = 13, 13 Hz, H-12), 3.94 (1H, dd, J = 5, 12 Hz, H-10), 2.25 (1H, m, H-9), 1.79 (1H, ddd, J = 3,13,13 Hz, H-8α), 1.54 (1H, ddd, J = 3, 3, 13 Hz, H-8β), 2.05 (1H, m, H- 6), 2.35 (1H, m, H-5), 5.54 (1H, brs, H-4), 4.82 (1H, brs, H-2), 3.43 (1H, dd, J = 8, 8 Hz, H-1β), 4.06 (1H, dd, J = 8, 8 Hz, H-1α),; 13C - NMR ($CDCl_3$, 150 MHz) δ 31.58 (q, C-15), 18.65 (q, C-14), 22.59 (q, C-13), 71.70 (d, C-12), 41.64 (s, C-11), 66.95 (d, C- 10), 33.36 (d, C-9), 38.22 (t, C-8), 78.61 (s, C-7), 52.47 (d, C-6), 26.96 (d, C-5), 121.77 (d, C-4), 142.57(s, C- 3), 70.74 (d, C-2), 72.69 (t, C-1). Spectroscopy data corresponds most with data in Vairappan and Tan (2005).

Aplysistatin (**2**)—white crystal; $C_{15}H_{23}O_3Br$; ^{1}H-NMR ($CDCl_3$, 600 MHz) δ (3H, s, H-15), 0.96 (3H, s, H-14), 1.17 1.29 (3H, s, H13), 3.92 (1H, dd, J = 4, 14 Hz, H-10), 2.11 (1H, m, H-9), 2.28 (1H, m, H-9), 1.61 (lH, ddd, J = 3, 3, 13 Hz, H-8α), 1.79 (1H, ddd, J =3,13,13 Hz, H-8β), 2.04 (1H, m, H-6), 2.56 (1H, m, H-5), 6.96 (1H, brs, H-4), 5.13 (1H, brs, H-2), 3.87 (1H, dd, J = 8, 8 Hz, H-1α), 4.49 (1H, dd, J = 8, 8 Hz, H-lβ); 13C-NMR (CDCl3 150 MHz) δ 31.42 (q, C-15), 18.66 (q, C-14), 22.40 (q, C-13), 169.86 (s, C-12), 41.67 (s, C-11), 65.80 (d, C-10), 33.09 (d, C-9), 38.32 (t, C-8), 79.72 (s, C-7), 51.90 (d, C-6), 27.87 (d, C-5), 143.81 (d, C-4), 132.59 (s, C-3), 67.45 (d, C-2), 70.56 (d, C-1). Spectroscopy data corresponds most with data in Vairappan and Tan (2005).

5-Acetoxypalisadin B (**3**)—oil; $C_{17}H_{26}O_3Br_2$; $_1$H-NMR ($CDCl_3$, 600 MHz) δ 1.22 (3H, s, H3-15), 1.03 (3H, s, H3-14), 1.65 (3H, s, H13), 1.61 (1H, m, H-8α), 1.77 (3H, s, H3-12), 1.86 (1H, m, H-8β), 2.10 (3H, s, H3-16), 3.88 (1H, dd, J = 4, 13 Hz, H-10), 2.18 (1H, m, H-9a), 2.31 (1H, m, H-9β), 1.75 (1H, m, H-6), 5.80 (1H, d, J = 8 Hz, H-5), 5.71 (1H, d, J = 6 Hz, H-4), 4.45 (1H, d, J = 9 Hz, H-2), 3.43 (1H, dd, J = 8 Hz, 11 Hz, H-1α), 3.72 (1H, dd, J = 3, 11 Hz, H-1β); 13C - NMR (CDCl3, 150 MHz) δ 171.10 (C-17), 22.22 (C-16), 31.58 (q, C-15), 19.45 (q, C-14), 25.99 (q, C-13), 21.91 (q, C-12), 42.09 (s, C-11), 66.80 (d, C-10), 33.51 (d, C-9), 40.09 (t, C-8), 78.62 (s, C-7), 54.56 (d, C-6), 70.43 (d, C-5), 127.72 (d, C-4), 143.25 (s, C-3), 70.87 (d, C-2), 35.50 (t, C-1). Spectroscopy data corresponds most with data in Vairappan and Tan (2005).

Spectrometry analysis

We further analysed the extract of *L.snackeyi* using mass spectrometry. A total of 37 metabolites; 30 from positive mode and 7 from negative mode were identified putatively via high resolution tandem mass spectrometry profiling (Table 1). These 37 metabolites mainly comprised of fatty acids (9), terpenoids (7), phenolics (4), aromatics (4), and cyclic ketones (3). Among the terpenoids, four steroids and one pentacyclic triterpenoid were detected. However, their putative identities were masked as the identification of these underivatized compounds via tandem mass spectrometry could be misleading. The main reason is that their multi-ring skeleton possess diverse stereoisomerisms and do not yield sufficient product ions species for detail identification (Murphy 2015). Figures 5 and 6 compiles the chemical structures for the LCMS detected metabolites.

Molecular docking studies

Molecular docking studies were conducted to investigate the cholinesterase inhibitory properties of *L. snackeyi* metabolites based on the inhibitory effects on the AChE and BChE proteins. For a metabolite to be regarded optimally docked, as compared to a reference, a recommended RMSD value and S-score of lower than 2Å and and −7 kcal/mol, respectively were considered. Table 1 lists the docking results for all metabolites that fulfilled the criteria along with a reference ligand. Molecular docking data for all 33 metabolites are provided in Supplementary Tables 1 and 2.

Protein-ligand interaction with AChE.

The molecular docking of the reference ligand, galantamine with AChE recorded the *S*-score of −−7.47 kcal/mol. The *L. snackeyi* metabolites recorded *S*-scores that ranged from −4.60 to −8.72 kcal/mol. A total of 12 candidates recorded *S*-score values of −7 kcal/mol and lower. Ten candidates, docosahexaenoic acid (**30**), 5,8,11,14-eicosatetraynoic Acid (**31**), 2,7,12,17-octadecanetetrol (**32**), erucamide (**34**), 6-gingerol (**39**), 15-hydroxy-1-[2-(hydroxymethyl)-1-piperidinyl] prost-13-ene-1,9-dione (**42**), 8-[3-oxo-2-(2-penten-1-yl)-1-cyclopenten-1-yl]octanoic acid (**43**), 15-oxo-11,13-eicosadienoic acid (**50**), 9,12,13-trihydroxy-15-octadecenoic acid (**53**) and oleic acid (**54**) recorded strong binding with low S-scores ranging from -7.54 kcal/mol to −8.72 kcal/mol. However, taking into consideration of the RMSD value, 5,8,11,14-eicosatetraynoic acid (31) (−8.72 kcal/mol) had the lowest RMSD value of 1.53 Å among the ten

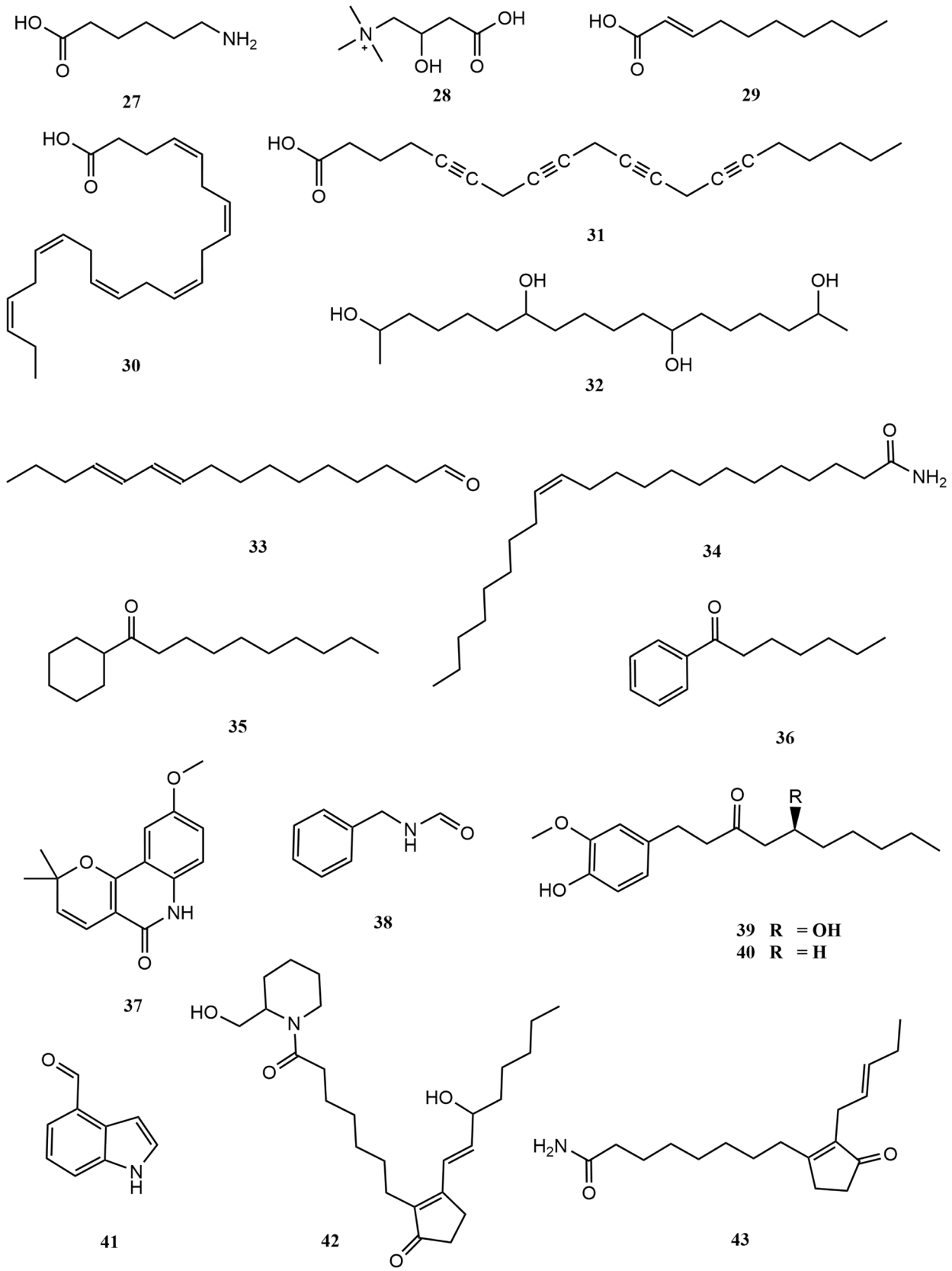

Fig. 5 Structures of *L. snackeyi* metabolites detected through MS analysis as reported in Table 1

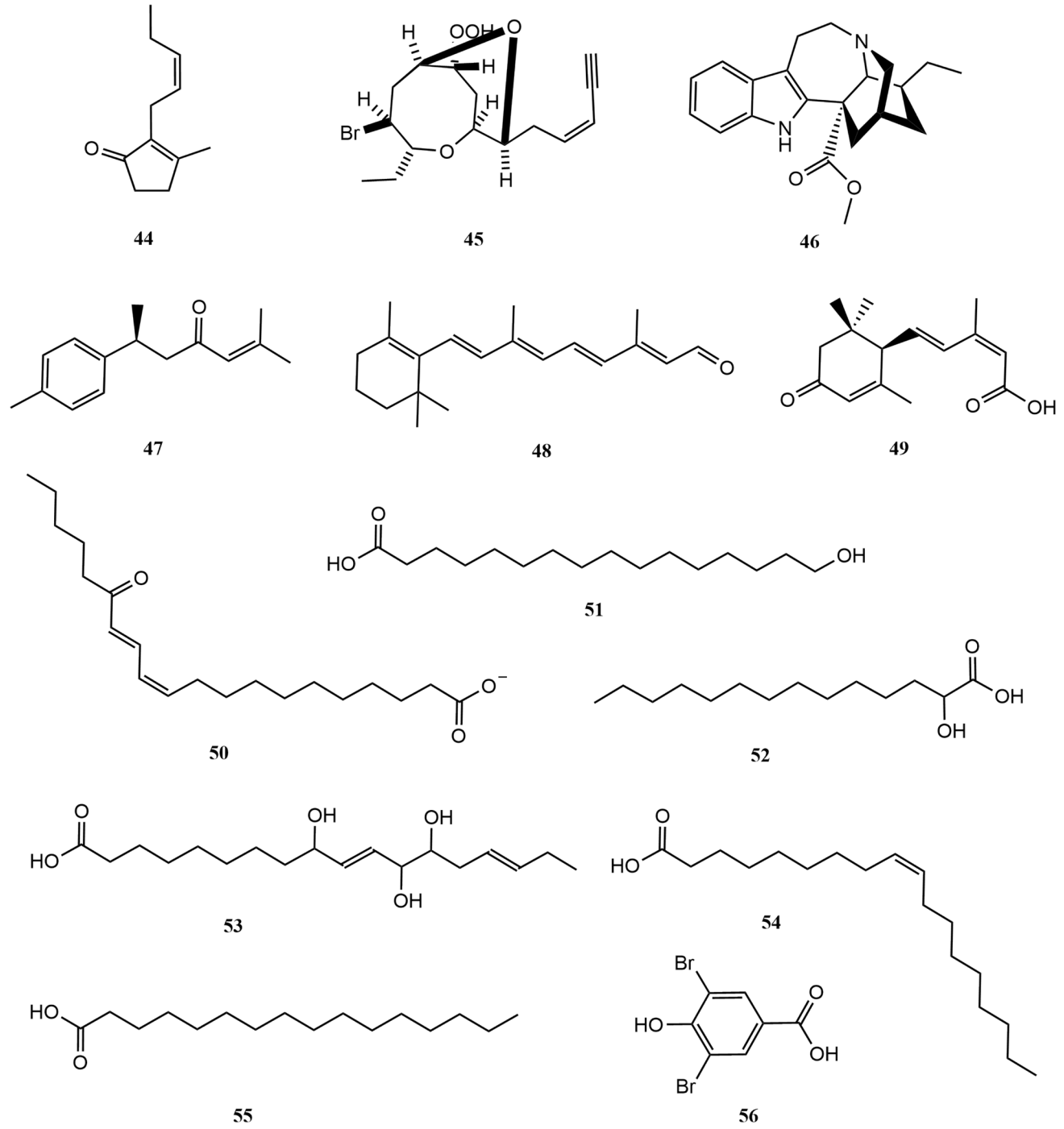

Fig. 6 Structures of *L. snackeyi* metabolites detected through MS analysis as reported in Table 1 (cont.)

metabolites, making it a potential inhibitor against the acetylcholinesterase enzyme.

The reference ligand, galantamine formed one conventional hydrogen bond, one carbon hydrogen bonds, and fifteen (15) van der Waals interactions with AChE, as recorded in Table 2. Figure 7 shows that the reference ligand formed hydrogen bond with amino acid residues at Glu202, with Glu202 being an amino acid residue from the binding site. The reference ligand also formed carbon hydrogen bond with Tyr337 and van der Waals interactions

Table 1 Putatively identified metabolites from positive and negative mode of MS/MS analysis

Metabolites	Formula	Mass error (ppm)	*m/z*	Class	Bioactivity	References
Putatively identified metabolites from positive mode of MS/MS analysis						
6-Aminocaproic acid (**27**)	$C_6H_{13}NO_2$	−0.05	132.1019	Amino acid	Antifibrinolytic	(Ferreira et al. 2021; Srivastava et al. 2019)
Carnitine (**28**)	$C_7H_{15}NO_3$	−0.93	162.1123	Amino acid	Fatty acid oxidation for energy conversion	(Ghoran et al. 2021)
2-Decenoic acid (**29**)	$C_{10}H_{18}O_2$	−0.64	171.1379	Fatty acid	Biofilm control	(Tripathi et al. 2019; Kabir et al. 2021)
Docosahexaenoic acid (**30**)	$C_{22}H_{32}O_2$	−1.05	329.2472	Fatty acid	Anti-inflammation; cell signalling; cell proliferation	(Hu et al. 2023; Abduljelil et al. 2022)
5,8,11,14-Eicosatetraynoic acid (**31**)	$C_{20}H_{24}O_2$	−1.14	297.1846	Fatty acid	Anti-inflammation; antipyretic	(Palaniveloo and Vairappan 2014)
2,7,12,17-Octadecanetetrol (**32**)	$C_{18}H_{38}O_4$	−1.68	319.2838	Fatty alcohol		
10,12-Hexadecadienal (**33**)	$C_{16}H_{28}O$	−1.07	237.2210	Fatty aldehyde		
Erucamide (**34**)	$C_{22}H_{43}NO$	−1.55	338.3412	Fatty amide	Acetylcholinesterase inhibitor; antidepressant; antimicrobial	(Vairappan et al. 2004; Kamada and Vairappan 2012; Masuda et al. 1997)
Decanophenone (**35**)	$C_{16}H_{24}O$	−0.22	233.1899	Aromatic ketone		
Heptanophenone (**36**)	$C_{13}H_{18}O$	−0.27	191.1430	Aromatic ketone		
Haplamine (**37**)	$C_{15}H_{15}NO_3$	−1.71	258.1120	Pyranoquinoline alkaloid	Cytotoxic; antifungal; antialgal	(Ellman et al. 1961; Aristyawan et al. 2022)
N-Benzylformamide (**38**)	C_8H_9NO	−0.28	136.0757	Aromatic formamide		
11-(2-Hexyl-5-hydroxyphenoxy)-N-(2-hydroxyethyl) undecanamide	$C_{25}H_{43}NO_4$	−1.25	422.3260	Phenolic		
6-Gingerol (**39**)	$C_{17}H_{26}O_4$	−0.99	295.1901	Phenolic	Cytotoxic; analgesic; anti-oxidation; anti-inflammation	(Chang et al. 2023; Zhan et al. 2023; Maran et al. 2021)
Paradol (**40**)	$C_{17}H_{26}O_3$	−0.13	279.1954	Phenolic	Cytotoxic; anti-inflammation; neuroprotective; antidiabetic	(Hastings et al. 2016; Davies et al. 2015; Mendez et al. 2019; Sud et al. 2006)
Indole-4-carboxaldehyde (**41**)	C_9H_7NO	0.13	146.0601	Indole	Anti-inflammation	(Cheung et al. 2012)
15-Hydroxy-1-[2-(hydroxymethyl)-1-piperidinyl]prost-13-ene-1,9-dione (**42**)	$C_{26}H_{45}NO_4$	−0.57	436.3419	Cyclic ketone		
8-[3-Oxo-2-(2-penten-1-yl)-1-cyclopenten-1-yl]octanoic acid (**43**)	$C_{18}H_{28}O_3$	−1.15	293.2108	Cyclic ketone		
Jasmone (**44**)	$C_{11}H_{16}O$	0.49	165.1275	Cyclic ketone	Plant-defence activator; anti-inflammation	(Nachon et al. 2013; Khelfaoui et al. 2021)
Laurendecumenyne A (**45**)	$C_{15}H_{21}BrO_4$	−0.23	345.0695	Acetogenin		(Vairappan and Tan 2005)
Coronaridine (**46**)	$C_{21}H_{26}N_2O_2$	−0.57	339.2065	Alkaloid	Antiparasite; cytotoxic	(Murphy 2015; Brown et al. 2018)
ar-Turmerone (**47**)	$C_{15}H_{20}O$	0.21	217.1587	Sesquiterpenoid	Antiplatelet; anti-angiogenesis; cytotoxic; anti-inflammation; anti-depression	(Coleman et al. 2021; Brass 2000; Jennings et al. 2012; Marques et al. 2015)
Retinaldehyde (**48**)	$C_{20}H_{28}O$	−1.21	285.2210	Vitamin A	Visual-essential metabolite; antimicrobial; adipogenesis inhibitor	(Niemoller and Bazan 2010; Salem et al. 2001)
Abscisic acid (**49**)	$C_{15}H_{20}O_4$	1.89	265.1428	Phytohormone		(Stuhlmeier et al. 1997)
Steroidal compound	$C_{46}H_{78}N_2O_5$	0.05	739.5984	Steroid		

Table 1 (continued)

Metabolites	Formula	Mass error (ppm)	*m/z*	Class	Bioactivity	References
Steroidal compound	$C_{19}H_{28}O_3$	−0.91	305.2109	Steroid		
Steroidal compound	$C_{27}H_{44}O$	−1.50	385.3459	Steroid		
Steroidal compound	$C_{27}H_{42}$	−0.72	367.3357	Steroid		
Pentacyclic compound	$C_{48}H_{82}N_2O_5$	−0.41	767.6293	Triterpenoid		
Putatively identified metabolites from negative mode of MS/MS analysis						
15-oxo-11,13-Eicosadienoic acid (**50**)	$C_{20}H_{34}O_3$	0.32	321.2436	Fatty acid		
16-Hydroxypalmitic acid (**51**)	$C_{16}H_{32}O_3$	0.02	271.2279	Fatty acid		
2-Hydroxymyristic acid (**52**)	$C_{14}H_{28}O_3$	−0.58	243.1964	Fatty acid	Antiviral	(Li et al. 2017)
9,12,13-Trihydroxy-15-octadecenoic acid (**53**)	$C_{18}H_{34}O_5$	0.99	329.2337	Fatty acid		
Oleic Acid (**54**)	$C_{18}H_{34}O_2$	−1.76	281.2481	Fatty acid	Antidiabetic; anti-inflammation	(Kim et al. 2018; Xie et al. 2021)
Palmitic Acid (**55**)	$C_{16}H_{32}O_2$	−1.24	255.2326	Fatty acid	Antitumor; pro-inflammation; pro-apoptotic	(Cantrell et al. 2005; Ea et al. 2008; Dugasani et al. 2010)
3,5-Dibromo-4-hydroxybenzoic acid (**56**)	$C_7H_4Br_2O_3$	0.26	292.8455	Phenolic		

with Gly120, Gly121, Gly122, Tyr124, Ser125, Tyr133, Ser203, Ala204, Trp236, Phe295, Phe297, Tyr341, His447, Gly448 and Ile451. As compared to the reference ligand, 5,8,11,14-eicosatetraynoic acid (**31**) formed one conventional hydrogen bond, two carbon-hydron bonds, and eighteen (18) van der Waals interactions. The metabolite formed conventional hydrogen bonds with the amino acid residues at Tyr133 and carbon hydrogen bonds with Gly121 and Gly126 (Fig. 7). The metabolite also exhibited van der Waals interactions with Asp74, Asn87, Tyr119, Gly120, Gly122, Tyr124, Ser125, Ala127, Leu130, Glu202, Ser203, Als204, Trp286, Phe297, Phe338, Tyr341, His447 and Gly448. The protein-ligand interaction can be seen in Fig. 7.

Protein-ligand interaction with BChE

The molecular docking of the reference ligand, tacrine with BChE recorded an *S*-score of −5.98 kcal/mol. The *L. snackeyi* metabolites were docked with *S*-scores ranging from −4.81 to −8.69 kcal/mol and a total of fourteen (14) candidates recording *S*-score values of −7 kcal/mol and lower. From the total of 33 metabolites tested, docosahexaenoic acid (**30**), 5,8,11,14-eicosatetraynoic acid (**31**), 2,7,12,17-octadecanetetrol (**32**), 10,12-hexadecadienal (**33**), erucamide (**34**), decanophenone (**35**), 6-gingerol (**39**), paradol (**40**), 15-hydroxy-1-[2-(hydroxymethyl)-1-piperidinyl] prost-13-ene-1,9-dione (**42**), 8-[3-oxo-2-(2-penten-1-yl)-1-cyclopenten-1-yl]octanoic acid (**43**), retinaldehyde (**48**), 15-oxo-11,13-eicosadienoic acid (**50**), 9,12,13-trihydroxy-15-octadecenoic acid (**53**) and oleic acid (**54**) showed strong binding with low S-score ranging from −7.05 to −8.69 kcal/mol. 15-Hydroxy-1-[2-(hydroxymethyl)-1-piperidinyl] prost-13-ene-1,9-dione (**42**) exhibited the lowest S-score -8.69 kcal/mol and had a good RMSD value of 1.78 Å making it the best candidate to inhibit the butyrylcholinesterase enzyme.

The reference ligand, tacrine was found to form one conventional hydrogen bond and thirteen (13) van der Waals interactions with BChE, as shown in Table 1. Figure 8 shows that the reference ligand formed hydrogen bonds with amino acid residues from the binding site at His438. The reference ligand also formed van der Waals interactions at Asp70, Gly78, Ser79, Gly116, Gly117, Thr120, Tyr128, Ser198, Tyr332, Met437, Gly439, Tyr440, and Ile442. As compared to the reference ligand, 15-hydroxy-1-[2-(hydroxymethyl)-1-piperidinyl]prost-13-ene-1,9-dione (**42**) formed a carbon hydrogen bond and twenty (20) van der Waals interactions with BChE. 15-Hydroxy-1-[2-(hydroxymethyl)-1-piperidinyl]prost-13-ene-1,9-dione (**42**) formed carbon hydrogen bonds at Gly116, while also displaying van der Waals interactions at Asp70, Ser79, Asn83, Gly115, Gly117, Gln119, Thr120,

Table 2 Molecular docking results of *Laurencia snackeyi* metabolites with Acetylcholinesterase (AChE) and Butyrylcholinesterase (BChE) protein

Compound number	*S*-score (kcal/mol)	RMSD (Å)	H bond	Van der Waals	C–H bond	Amino acid residue (H bond)
Acetylcholinesterase (AChE)						
Galantamine	− 7.47	1.06	1	15	1	*Glu202
31	− 8.72	1.53	1	18	2	Tyr133
42	− 8.22	3.88	2	23	1	Ser293; Tyr341
34	− 8.13	1.81	2	23	0	Trp286; Ser293
30	− 7.97	1.79	0	19	0	–
50	− 7.80	0.96	2	21	1	Val294
43	− 7.80	2.08	2	21	1	*Trp86; Tyr341
53	− 7.73	1.70	2	15	1	*Glu202; *Phe295
39	− 7.73	1.92	1	19	2	*Glu202
32	− 7.69	1.88	2	21	1	Tyr34; Tyr124
54	− 7.54	1.59	1	21	0	Ser125
Butyrylcholinesterase (BChE)						
Tacrine	− 5.98	3.60	1	13	0	–
42	− 8.69	1.78	0	20	1	–
30	− 8.07	1.45	3	19	0	Gly116; Gly117; Ser198
34	− 7.75	1.17	1	21	0	Gln71
31	− 7.73	1.67	3	21	0	Gly117; Ser198; Ala199
53	− 7.55	4.86	4	16	0	Gly116; Ser198; Ser198; *His438
50	− 7.40	2.66	2	16	1	Gly115; Gly116
39	− 7.34	1.25	1	16	2	Leu286
40	− 7.25	1.92	1	20	1	*Glu197
43	− 7.24	1.19	1	20	2	Leu286
54	− 7.24	2.51	3	22	0	Gly116; Gly117; Ser198

*Hydrogen bond formed with amino acid residues from binding site

Tyr128, Glu197, Ser198, Pro285, Ser287, Ala328, Phe329, Tyr332, Phe398, Met437, Gly439, Tyr440, and Ile442. The protein-ligand interaction can be seen in Fig. 8.

Discussion

Chemotaxonomic significance of *L.snackeyi* metabolites

Laurencia is well-known for their diverse halogenated metabolites, a characteristic unique to the genus (Kamada and Vairappan 2017). Since the discovery of *L. snackeyi*, a total of 26 sesquiterpenoids had been reported mostly from Malaysian and Okinawan waters (Table 3). The molecules are shown in Fig. 9. In the Malaysian waters, almost all *L. snackeyi* records were from locations in Sabah (North Borneo) and only one report was available from Peninsular Malaysia in 1997. A total of 11 metabolites have been reported from the Malaysian species that are palisadin A (**1**), aplysistatin (**2**), 5-acetoxypalisadin B (**3**), palisadin D (**4**), 15-hydroxypalisadin A (**5**), 5β-hydroxypalisadin B (**6**), 12-acetoxypalisadin B (**7**), 12-hydroxypalisadin B (**8**), palisadin B (**9**), 3,4-epoxypalisadin B (**10**) and 1,2-dehydro-3,4-epoxypalisadin B (**11**). Specifically, compound **1** and **2** was found consistently in all populations from Malaysia, Japan and Vietnam, while compound **3** has been reported in several populations. All these compounds are of the chemical skeleton synderane which has been suggested to be a chemotaxonomical marker to *L.snackeyi* (Palaniveloo and Vairappan 2014; Tan et al. 2011; Ishii et al. 2020; Wijesinghe et al. 2014).

Among other non-synderane metabolites reported from *L.snackeyi* in literature were debromolaurinterol (**12**), α-bromocuparene (**13**), snakeol (**14**), snakediol (**15**), palisol (**16**), 4-bromo-β-chamigren-8-one (**17**), 3,3-dimethyl-5-methylene-4-(3-methylpenta-2,4-dien-1-yl)cyclohex-1-ene (**18**), luzonensin (**19**), luzonensol acetate (**20**), chamigr-2,5(14)-dien-8-one (**21**), luzonensol (**22**), luzonenone (**23**), luzofuran (**24**), pacifigorgiol (**25**) and (3Z,6E)-1-bromo-3,7,11-trimethyl-3,6,10-dode-

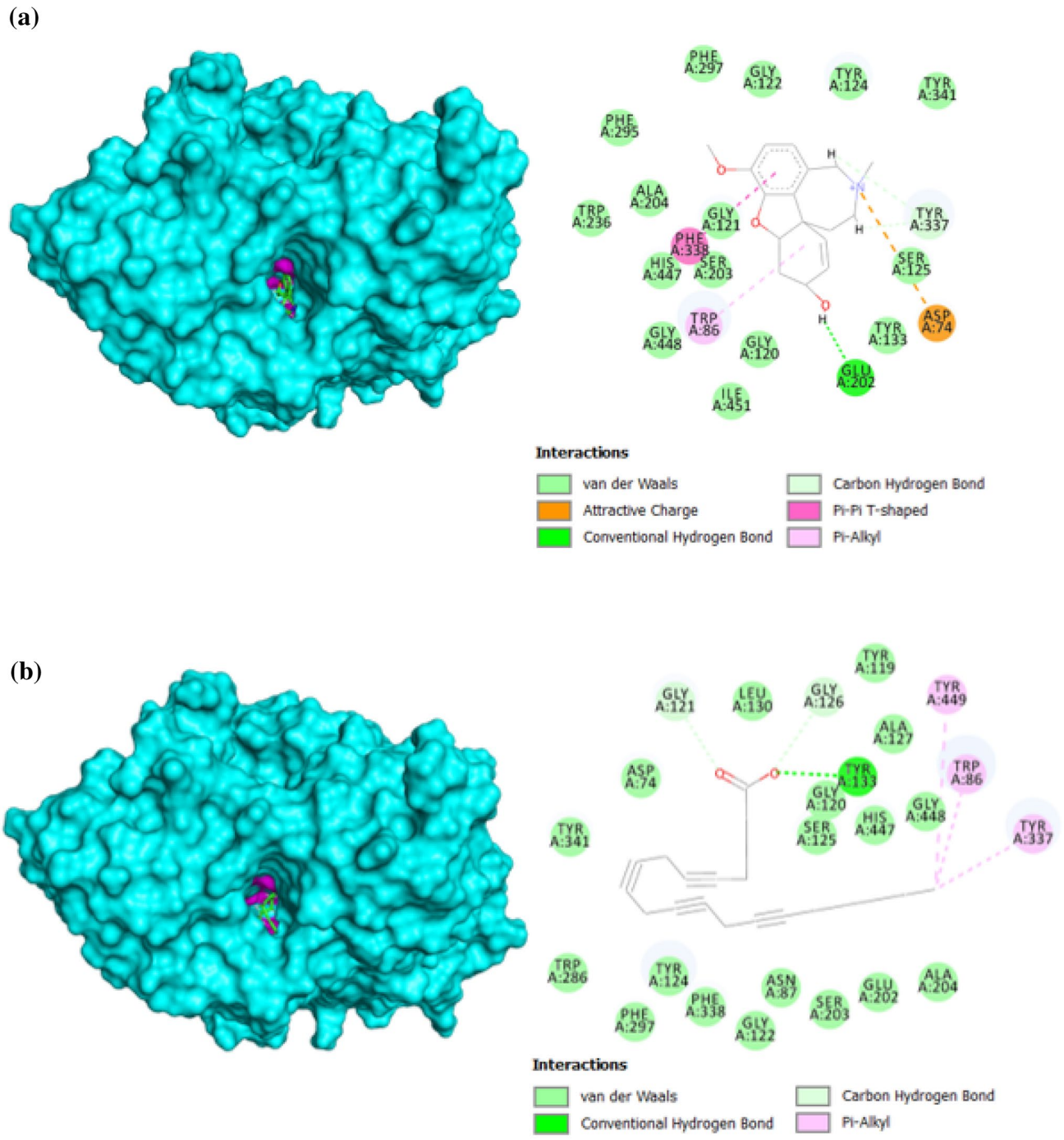

Fig. 7 The docking conformation of AChE with **a** galantamine; **b** 5,8,11,14-eicosatetraynoic acid (**31**)

catrien-2-ol (**26**). The chemical structures of all *L. snackeyi* metabolites are shown in Fig. 9.

Metabolites from the genus *Laurencia* have also been associated to as part of diet and defense mechanism (Palaniveloo et al. 2020) of these opisthobranch molluscs. This is very much attributed to the bioactivity of the compounds. The unique chemotaxonomy of the genus *Laurencia* has made it possible to determine the herbivory among sea hare species such as *Aplysia dactylomela* and *A. parvula*. Previously Palaniveloo and Vairappan (2014) reported palisadin A (**1**), aplysistatin (**2**) and 5-acetoxypalisadin B (**3**) from the *A. dactylomela*

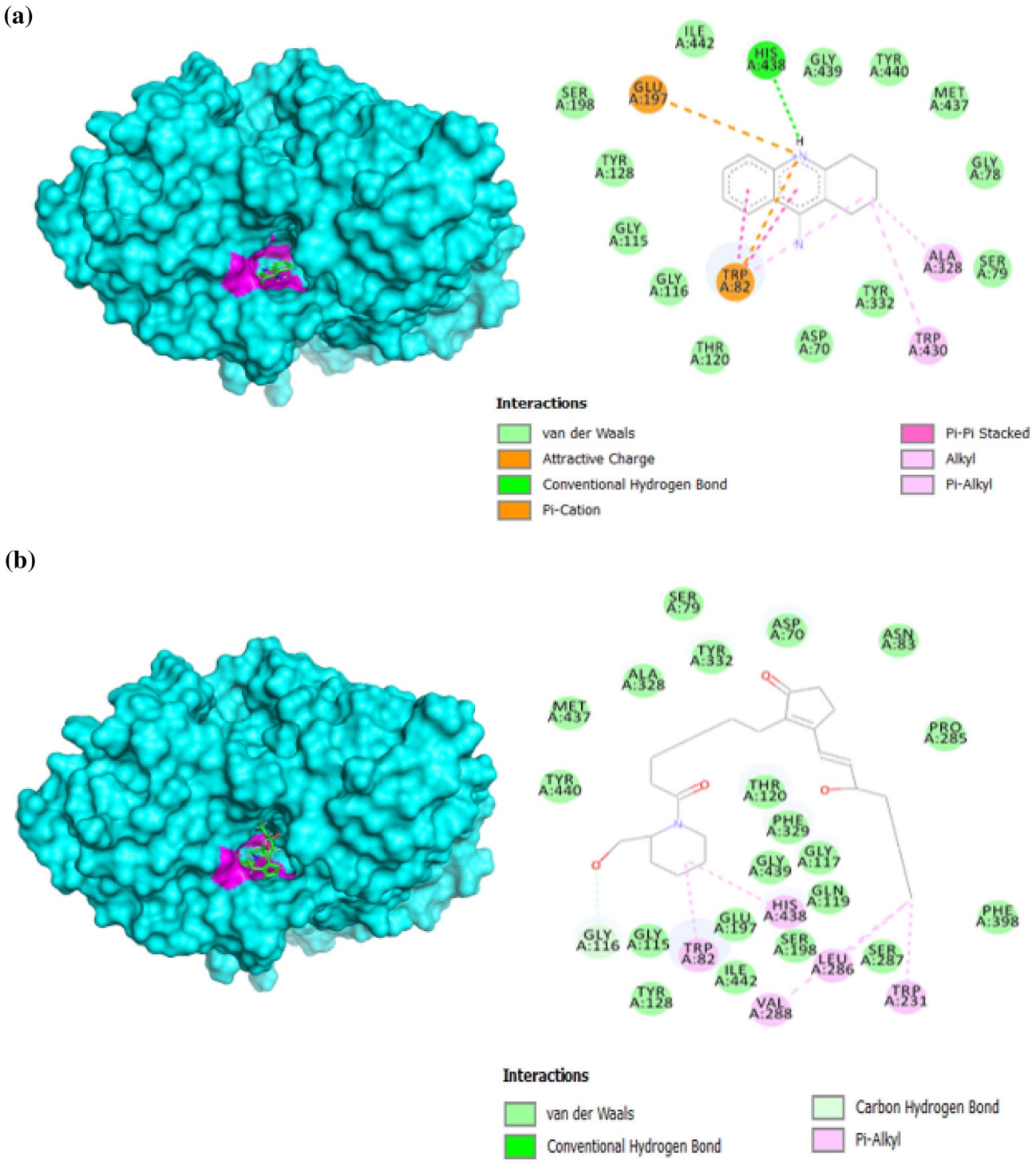

Fig. 8 The docking conformation of BChE with **a** tacrine; **b** 15-Hydroxy-1-[2-(hydroxymethyl)-1-piperidinyl]prost-13-ene-1,9-dione (**42**)

collected off the waters of Sulug Island in Borneo and was traced back to its diet, *L. snackeyi* Palaniveloo and Vairappan (2014). Similar finding was also reported by Vairappan and Tan (2005) and Vairappan et al. (2007) where 12-acetoxypalisadin B (**7**), 12-hydroxypalisadin B (**8**) and palisadin B (**9**) were isolated. Palisadin A (**1**) has also been reported from *A. parvula* from Borneo Vairappan et al. (2009). The established chemotaxonomy for *L.*

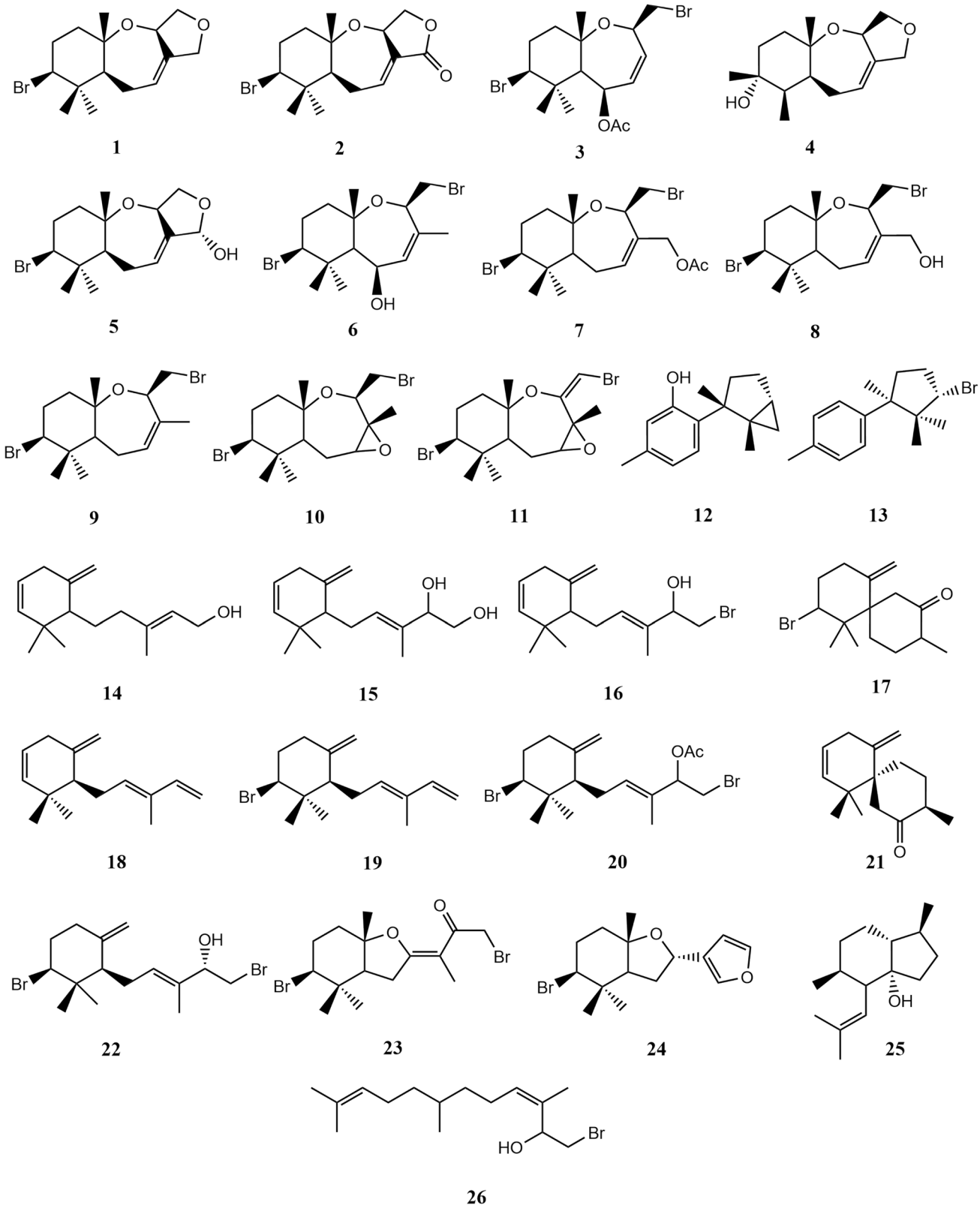

Fig. 9 Chemical structures of sesquiterpene type metabolites reported from *L. snackeyi*

Table 3 Summary of sesquiterpenoids from *L. snackeyi* from the tropical and sub-tropical waters

Country	Location	Metabolites	References
Malaysia	Port Dickson, Straits of Malacca	1, 2, 3	This study
	Mantanani Island, Sulug Island and Dinawan Island, Kota Kinabalu	1, 2, 3, 7, 9, 16, 18, 25	(Lee et al. 2008)
	Carrington Reef, Bak-Bak Beach and Lankayan, Sabah	1, 2, 3, 6, 9, 17, 21	(Young et al. 2005)
	Sepanggar, Kota Kinabalu	1, 2, 3, 16	(Gaire et al. 2015)
	Sulug Island, Kota Kinabalu	6, 9, 16, 25	(Hattori et al. 2012)
	Bum Bum Island, Semporna	1, 3, 4, 9, 12, 13, 14, 15, 16, 18, 25	(Lee and Surh 1998)
	Pulau Besar, Melaka; Sipanggau Island, Semporna; Manukan Island, Kota Kinabalu	1, 2, 3	(Wei et al. 2017)
Japan	Okinawa	1, 2, 9, 16, 18, 19, 20, 22, 25, 26	(Cha et al. 2019)
	Kukada Island, Okinawa	5, 10, 11, 22, 23, 24	(de Moura Fé et al. 2022)
	Okinawa	1, 2, 8, 9, 12, 13, 18, 22	(Moraes et al. 2008)
Vietnam	Phu Quoc Island	1, 2	(Wei et al. 2017)

snackeyi has made it possible to confirm the identity of the red algae species in Port Dickson, as reported in this manuscript.

Diversity of metabolites in investigated *L.snackeyi*

The *L.snackeyi* extract from this study which was subjected to HPLC profiling coupled with a PDA and scanned from 190 to 800 nm wavelength range. Previous reports reported the isolation of compounds from *L. snackeyi* between 220 and 254 nm due to the degrees of unsaturation in the metabolites (Palaniveloo and Vairappan 2014). This led to the isolation of prominent peaks detected in the extracts between UV wavelengths of 190 and 254 nm. Isolated peaks were subjected to NMR spectroscopy and the proton and carbon data were compared to available literature and three major isolates were identified as Palisadin A [**1**], Aplysistatin [**2**] and 5-acetoxypalisadin B [**3**]. Due to low yield for further isolation, we were determined to identify other available metabolites in the extract through LCMS profiling.

To the best of our knowledge, there has been no prior report on the mass spectrometry analysis of *L. snackeyi* crude extract. All existing publications reports isolated compounds. Our analysis detected 37 metabolites; 30 from positive mode and 7 from negative mode that were identified putatively *via* high resolution tandem mass spectrometry profiling and comprised of fatty acids (9), terpenoids (7), phenolics (4), aromatics (4), and cyclic ketones (3). However, only 32 detection were successfully confirmed and did not include the isolated metabolites **1**–**3**. This is probably due to limited databases related to marine metabolites. From our LCMS analysis, many of the detected metabolites was either cytotoxic or exhibit anti-inflammatory properties. Some of the notable detection from the LCMS data was the 6-aminocaproic acid (**27**) which is a derivative and analogue of lysine, which makes it an inhibitor for enzymes. 6-Aminocaproic acid (**27**) is reported as an antifibrinolytic agent that acts by inhibiting plasminogen activators which have fibrinolytic properties (Brown et al. 2018). Carnitine (**28**), an amino acid which contributes to the conversion fat through oxidation (Brass 2000) was also detected.

Fatty acids are an essential component of tissue and as many as twelve (12) fatty acids and its derivative (**29–33**, **50–55**) were recorded. Fatty acids and its derivatives are known to exhibit a range of bioactivities with anti-inflammation being most common, followed by anti-viral, anti-diabetic and anti-tumor (Jennings et al. 2012; Marques et al. 2015; Niemoller and Bazan 2010; Salem et al. 2001; Stuhlmeier et al. 1997; Li et al. 2017; Kim et al. 2018; Xie et al. 2021; Harper et al. 1996; Obici et al. 2002; Palomer et al. 2018; Ghezzal et al. 2020; Lu et al. 2003; Zhu et al. 2021). Erucamide (**34**), classified as a slip agent that has anti-biofouling properties is not surprising to be part of the algal chemical list given the almost slimy surface of *L.snackeyi* that prevents fouling (Getachew et al. 2016). Kim et al. (2018) reported that the pre-treatment of mice with erucamide significantly prevented memory deficits suggesting its potential to aid in Alzheimer's disease by modulation of cholinergic functions (Kim et al. 2018). Haplamine (**37**) is an alkaloid that had been reported to exhibit anti-fungal properties. The MS detection of 6-gingerol (**39**), paradol (**40**) and ar-turmerone (**47**) in the extract of *L.snackeyi* raised eyebrows since these metabolites are common constituents causing the pungent smell in gingers. Indole-4-carboxaldehyde (**41**) was previously reported from the seaweed *Sargassum thunbergii* as an anti-inflammatory agent in MGO-induced inflammation in HepG2 cells (Cha et al. 2019).

Jasmone (**44**) is a volatile organic found in flowers or leaves of several plant species and acts as an attractant for pollinators and as a chemical cue for host localization for insects. In some reports, jasmones play a role as deterrent to pests (Moraes et al. 2008). As such, it is possible in *L.snackeyi*, this volatile plays are role in defence against herbivory. The detection of the acetogenin laurendecumenyne A (**45**) was also an interesting finding. The only previous report on the acetogenin is from *L.decumbens* from China (2007) Ji et al. (2007). Acetogenins from algae are quite different from plant acetogenins. They are usually halogenated, and have an enyne or a bromoallene terminal group (Wanke et al. 2015). Acetogenins are proposed as chemotaxonomic markers for *L.nangii* (Suzuki and Vairappan 2005). Abscisic acid (**49**) is a phytohormone that regulates the oxidative stress state under desiccation in seaweed species (Gomez-Cadenas et al. 2015). A wide range of bioactivity is often associated to the presence of halogens and benzene rings. Bromophenols (BPs) are such compounds detected in the *L. snackeyi* extract. 3,5-Dibromo-4-hydroxybenzoic acid (**56**) is a BP with a benzene ring with two bromines and hydroxyl-substituents. The ecological function of BPs is not yet clear, but its role in chemical defense and deterrence is highly suspected (Liu et al. 2011).

In vitro cholinesterase inhibition

Plenty of attention has been given to macroalgae for the development of new drugs, nutraceuticals, and dietary supplements due to the characteristics of macroalgae as anti-inflammatory, antioxidant, anti-tumor, anti-diabetic, and antibacterial agents. There are also evidence that macroalgal-derived compounds are capable of improving neurodegenerative conditions. A review on the potential neuroprotective compounds from macroalgae reported that between 1999–2004, Ochrophyta (class Phaeophyceae) contributed 57 compounds of the total, followed by 28 from Rhodophyta and 14 compounds Chlorophyta. Alzheimer's associated metabolites had been reported from the red algae *Gloiopeltis furcata* where phlorotannins were the most prominent chemical class of cholinesterase inhibitors, followed by sterol, terpene and fatty acids (Alghazwi et al. 2016). The compounds reported from red algae genus *Laurencia* has long been associated to various bioactivities. Being halogenated in nature increases the chances for the metabolites produced to exhibit bioactivity (Vairappan et al. 2013; Palaniveloo et al. 2020; Alghazwi et al. 2016). Compounds **1** and **2** are the main components that can be obtained from *L.snackeyi* and these compounds have been associated to a wide range of bioactivity such as anti-bacterial (Vairappan et al. 2009), anti-inflammatory (Vairappan et al. 2013), cytotoxicity (Avila and Angulo-Preckler 2020). So far, the charmigranes (-)-elatol, (-)-dendroidol and (-)-cartilagineol, sesquiterpenes isolated from the Brazilian *L. dendroidea* were the only *Laurencia* derived metabolites reported with 78.5%, 72.9%, and 61.3% AChE inhibiting potential, respectively. With reference to (-)-elatol, its activity is suspected to be resulted from the interaction between the bromine and chlorine with the benzene ring center of Trp86 and Trp286, as observed during molecular docking analysis (Gonçalves et al. 2020). Given the vast bioactive potential of *L. snackeyi*, there has been no prior investigation on the Alzheimer's related potential of this red algae. In fact, to date, there are no approved Alzheimer's disease drug from a marine source making it more exciting for in depth investigation.

Molecular docking of cholinesterase inhibitors

The development of computational techniques for drug discovery facilitates the quick virtual bioactivity screening of molecules. The docking aims to anticipate the affinity strength between receptor proteins and ligands (Pinzi and Rastelli 2019), therefore increasing the likelihood of locating a suitable drug candidates. This reduces the early costs associated with hit detection. The *S*-score and RMSD determine the interaction between ligand and receptor protein. The more negative the *S*-score, the stronger the interaction (Xu et al. 2018). However, an optimal condition would be a combination of RMSD value that is below 2Å with an *S*-score lower than −7 kcal/mol (Khelfaoui et al. 2021).

The acetylcholinesterase (AChE, PDB ID = 4EY6) and butyrylcholinesterase (BChE, PDB ID = 4BDS) enzyme were selected as these deactivate the neurotransmitter acetylcholine (ACh) that causes the promotion of Alzheimer's disease characterized by cholinergic deficiency (Greig et al. 2005; Kamada and Vairappan 2017; Viayna et al. 2020). Initial molecular docking for isolated compounds palisadin A (**1**), aplysistatin (**2**) and 5-acetoxypalisadin B (**3**) revealed weak potential as a cholinesterase inhibitor therefore was not the source of bioactivity in the in vitro assay. We proceeded to conduct a thorough investigation on the LCMS detected metabolites. The computational molecular docking of both the AChE and BChE receptors identified 5,8,11,14-eicosatetraynoic acid (**31**) and 15-hydroxy-1-[2-(hydroxymethyl)-1-piperidinyl]prost-13-ene-1,9-dione (**42**), respectively as the best cholinesterase inhibitors in the algae with optimal combination of *S*-score and RMSD values. There has been no prior information on the cyclic ketone **42**. However, there has been studies done on the role of ketones in neurodegenerative disease. The low *S*-value of 15-Hydroxy-1-[2-(hydroxymethyl)-1-piperidinyl]prost-13-ene-1,9-dione (**42**) could possibly be attributed to the presence of the piperidine ring which is also found present in the existing anti-Alzheimer's drug, donepezil (Tripathi et al. 2019). On the other hand, eicosatetraynoic acid (**31**) is a polyunsaturated fatty acid (PUFA). Several studies have highlighted the beneficial

effect of PUFAs against neurodegenerative diseases. These metabolites are primary components of the brain, thus associating it to membrane integrity and fluidity. As such PUFAs could act as a form of nutraceutical defence against brain related diseases. The red algae are generally important source of PUFAs and there has been existing report on the moderate effect on AChE inhibition (Barbosa et al. 2014). As previously mentioned, this research was restricted by low sample biomass which hindered in vitro and in vivo experiments. Which in silico experiments provides a prediction towards the potential of a metabolite, future investigations should include evaluating the actual potential of compounds to confirm its potential.

Conclusion

The discovery of *Laurencia snackeyi* as a new record in Terumbu Island shows that this genus is under documented in Malaysian waters creating a great opportunity for further investigation for ecology and drug discovery. The cholinesterase inhibitory activity of chemical constituents from the algal extract creates greater interest in the species as its potential source for Alzheimer's disease. This study confirms the potential of *L. snackeyi* and its metabolites as cholinesterase inhibitors through in vitro and in silico approaches. Nevertheless, this study is limited by the yield of extract and compounds for it to be evaluated via in vivo experiments. This indeed warrants more investigation and continuous research on the potential of halogenated metabolites as neurodegenerative disease agents.

Supplementary Information The online version contains supplementary material available at https://doi.org/10.1007/s13205-023-03725-6.

Acknowledgements Acknowledgements are due to the Marine Park Unit of Department of Fisheries, through Mr Albert Apollo Chan for organising and to the Expedition head, Dr Mohammed Rizman-Idid. We also convey our gratitude to Dr Yeong Hui Yin for the deposition of herbarium. This research is funded by the Science and Technology Research Partnership for Sustainable Development (SATREPS) Program entitled 'Development of Advanced Hybrid Ocean Thermal Energy Conversion (OTEC) Technology for Low Carbon Society and Sustainable Energy System: First Experimental OTEC Plant of Malaysia' funded by Japan Science and Technology Agency (JST) and Japan International Cooperation Agency (JICA), and Ministry of Higher Education Malaysia (MoHE) and led by the Institute of Ocean Energy Saga University (IOES) of Japan, and UTM Ocean Thermal Energy Centre (UTM OTEC), Universiti Teknologi Malaysia (UTM). Registered Program Cost Centre: R.K130000.7809.4L887, Project [Cost Centre: Project No IF045-2019]. This manuscript is also an output for the SATU Joint Research Scheme Grant between National Cheng Kung University (Project No. NCKU25) - Universiti Malaya (Project No. ST055-2021) and Universitas Airlangga (Project No. 1259/UN3.15/PT/2022) - Universiti Malaya (Project No. ST093-2022).

Author contributions Conceptualization, KP; methodology, KP, YYS, SS and HS; software, HS and JKT; validation, KP, SS, YYS, JKT and HS; formal analysis, KP, SS, YYS, JKT and HS; investigation, KP, SS, YYS, JKT and HS; resources, KP, SS OKH and HS; data curation, KP and SS; writing—original draft preparation, KP and OKH; writing—review and editing, KP, SS, OKH, SAR, PSM, MRI, SH, HSY; supervision, KP, SAR; project administration, KP; funding acquisition, SAR. All authors have read and agreed to the published version of the manuscript.

Availability of data and materials Raw data of known compounds NMR can be provided upon request.

Declarations

Conflict of interest The authors declare that they have no conflict of interest in the publication.

Ethics approval No human participants and/or animals were used in this publication.

Financial interest The authors declare they have no financial interest.

Consent to participate No human participants were used in this publication.

Consent for publication All authors have agreed for publication.

Code availability Not applicable.

References

Abduljelil A, Uzairu A, Shallangwa G, Abechi S (2022) In-silico design, molecular docking and pharmacokinetics studies of some tacrine derivatives as anti-Alzheimer agents: theoretical investigation. Adv J Chem Sect A 5:59–69

Alghazwi M, Kan YQ, Zhang W, Gai WP, Garson MJ, Smid S (2016) Neuroprotective activities of natural products from marine macroalgae during 1999–2015. J Appl Phycol 28:3599–3616

Aristyawan AD, Setyaningtyas VF, Wahyuni TS, Widyawaruyanti A, Ingkaninan K, Suciati S (2022) *In vitro* acetylcholinesterase inhibitory activities of fractions and iso-agelasine C isolated from the marine sponge *Agelas nakamurai*. J Res Pharm 26:279–286

Avila C, Angulo-Preckler C (2020) Bioactive compounds from marine heterobranchs. Mar Drugs 18:657

Barbosa M, Valentão P, Andrade PB (2014) Bioactive compounds from macroalgae in the new millennium: implications for neurodegenerative diseases. Mar Drugs 12:4934–4972

Brass EP (2000) Supplemental carnitine and exercise. Am J Clin Nutr 72:618–623

Brown S, Yao A, Taub PJ (2018) Antifibrinolytic agents in plastic surgery: current practices and future directions. Plast Reconstr Surg 141:937–949

Cantrell CL, Schrader KK, Mamonov LK, Sitpaeva GT, Kustova TS, Dunbar C, Wedge DE (2005) Isolation and identification of antifungal and antialgal alkaloids from *Haplophyllum sieversii*. J Agric Food Chem 53:7741–7748

Cha S-H, Hwang Y, Heo S-J, Jun H-S (2019) Indole-4-carboxaldehyde isolated from seaweed, *Sargassum thunbergii*, attenuates methylglyoxal-induced hepatic inflammation. Mar Drugs 17:486

Chang Y, Bai M, Zhang X, Shen S, Hou JY, Yao GD, Huang XX, Song SJ (2023) Neuroprotective and acetylcholinesterase inhibitory activities of alkaloids from *Solanum lyratum* Thunb.: an in vitro and in silico analyses. Phytochemistry 209:113623

Cheung J, Rudolph MJ, Burshteyn F, Cassidy MS, Gary EN, Love J, Franklin MC, Height JJ (2012) Structures of human acetylcholinesterase in complex with pharmacologically important ligands. J Med Chem 55:10282–10286

Coleman M, Davis J, Maher KO, Deshpande SR (2021) Clinical and hematological outcomes of aminocaproic acid use during pediatric cardiac ecmo. J Extra Corpor Technol 53:40–45

Davies M, Nowotka M, Papadatos G, Dedman N, Gaulton A, Atkinson F, Bellis L, Overington JP (2015) ChEMBL web services: streamlining access to drug discovery data and utilities. Nucleic Acids Res 43:612–620

de Moura Fé TC, de Castro Ribeiro AD, Melo JC, da Rocha Tomé A, Vieira-Neto AE, Silva ARA, de Oliveira LG, Campos AR (2022) cis-Jasmone: phytopharmaceutical potential for the treatment of skin inflammation. Rev Bras Farmacogn 32:440–446

Delorenzi JC, Freire-de-Lima L, Gattass CR, Costa DdA, He L, Kuehne ME, Saraiva EMB (2002) *In vitro* activities of iboga alkaloid congeners coronaridine and 18-methoxycoronaridine against *Leishmania amazonensis*. Antimicrob Agents Chemother 46:2111–2115

Dugasani S, Pichika MR, Nadarajah VD, Balijepalli MK, Tandra S, Korlakunta JN (2010) Comparative antioxidant and anti-inflammatory effects of [6]-gingerol, [8]-gingerol, [10]-gingerol and [6]-shogaol. J Ethnopharmacol 127:515–520

Ea S, Giacometti S, Ciccolini J, Akhmedjanova V, Aubert C (2008) Cytotoxic effects of haplamine and its major metabolites on human cancer cell lines. Planta Med 74:1265–1268

Ellman GL, Courtney KD, Andres V Jr, Featherstone RM (1961) A new and rapid colorimetric determination of acetylcholinesterase activity. Biochem Pharmacol 7:88–95

Ferreira JPS, Albuquerque HMT, Cardoso SM, Silva AMS, Silva VL (2021) Dual-target compounds for Alzheimer's disease: natural and synthetic AChE and BACE-1 dual-inhibitors and their structure-activity relationship (SAR). Eur J Med Chem 221:1–26

Gaire BP, Kwon OW, Park SH, Chun K-H, Kim SY, Shin DY, Choi JW (2015) Neuroprotective effect of 6-paradol in focal cerebral ischemia involves the attenuation of neuroinflammatory responses in activated microglia. PLoS One 10:0120203

Getachew P, Getachew M, Joo J, Choi YS, Hwang DS, Hong YK (2016) The slip agents oleamide and erucamide reduce biofouling by marine benthic organisms (diatoms, biofilms and abalones). Toxicol Environ Health Sci 8:342–348

Ghezzal S, Postal BG, Quevrain E, Brot PL, Seksik Leturque A, Thenet S, Carrière V (2020) Palmitic acid damages gut epithelium integrity and initiates inflammatory cytokine production. Biochim Biophys Acta Mol Cell Biol Lipids 1865:158530

Ghoran HS, Kijjoa A (2021) Marine-derived compounds with anti-Alzheimer's disease activities. Mar Drugs 19:410

Gomez-Cadenas A, Vives V, Zandalinas IS, Manzi M, Sanchez-Perez AM, Perez-Clemente MR, Arbona V (2015) Abscisic acid: a versatile phytohormone in plant signaling and beyond. Curr Protein Pept Sci 16:413–434

Gonçalves KG, Silva LL, Soares AR, Romeiro NC (2020) Acetylcholinesterase as a target of halogenated marine natural products from *Laurencia dendroidea*. AlgalRes 52:102130

Greig NH, Utsuki T, Ingram DK, Wang Y, Pepeu G, Scali C, Yu SQ, Mamczarz J, Holloway HW, Giordano T, Chen D, Furukawa K, Sambamurti K, Brossi A, Lahiri DK (2005) Selective butyrylcholinesterase inhibition elevates brain acetylcholine, augments learning and lowers Alzheimer β-amyloid peptide in rodent. Proc Natl Acad Sci USA 102:17213–17218

Harper DR, Gilbert RL, O'Connor TJ, Kinchington D, Mahmood N, Mcllhinney RAJ, Jeffries DJ (1996) Antiviral activity of 2-hydroxy fatty acids. Antiviral Chem Chemother 7:138–141

Hastings J, Owen G, Dekker A, Ennis M, Kale N, Muthukrishnan V, Turner S, Swainston N, Mendes P, Steinbeck C (2016) Chebi in 2016: improved services and an expanding collection of metabolites. Nucleic Acids Res 44:1214–1219

Hattori H, Mori T, Shibata T, Kita M, Mitsunaga T (2012) 6-paradol acts as a potential anti-obesity vanilloid from grains of paradise. Mol Nutr Food Res 65:2100185

Hu D, Jin Y, Hou X, Zhu Y, Chen D, Tai J, Chen Q, Shi C, Ye J, Wu M, Zhang H (2023) Application of marine natural products against Alzheimer's disease: past, present and future. Mar Drugs 21:43

Ishii T, Hisada W, Abe T, Kikuchi N, Suzuki M (2020) A new record of the marine red alga *Laurencia snackeyi* from Japan and its chemotaxonomic significance. Rec Nat Prod 14:150–153

Jennings JA, Courtney HS, Haggard WO (2012) Cis-2-decenoic acid inhibits *S. aureus* growth and biofilm *in vitro*: a pilot study. Clin Orthop Relat Res 470:2663–2670

Ji N-Y, Li X-M, Li K, Wang B-G (2007) Laurendecumallenes A-B and Laurendecumenynes A-B, Halogenated Nonterpenoid C_{15}-Acetogenins from the Marine Red Alga *Laurencia decumbens*. J Nat Prod 70:1499–1502

Kabir MT, Uddin MS, Jeandet P, Emran TB, Mitra S, Albadrani GM, Sayed AA, Abdel-Daim MM, Simal-Gandara J (2021) Anti-Alzheimer's molecules derived from marine life: understanding molecular mechanisms and therapeutic potential. Mar Drugs 19:251

Kamada T, Vairappan CS (2012) A new bromoallene-producing chemical type of the red alga *Laurencia nangii* Masuda. Molecules 17:2119–2125

Kamada T, Vairappan CS (2017) Non-halogenated new sesquiterpenes from Bornean *Laurencia snackeyi*. Nat Prod Res 31:333–340

Khelfaoui H, Harkati D, Saleh BA (2021) Molecular docking, molecular dynamics simulations and reactivity, studies on approved drugs library targeting ACE2 and SARS-CoV-2 binding with ACE2. J Biomol Struct Dyn 39:7246–7262

Kim CR, Kim HS, Choi SJ, Kim JK, Gim MC, Kim Y-J, Shin D-H (2018) Erucamide from radish leaves has an inhibitory effect against acetylcholinesterase and prevents memory deficit induced by trimethyltin. J Med Food 21:769–776

Kuniyoshi M, Marma MS, Higa T, Bernardinelli G, Jefford CW (2001) New bromoterpenes from the red alga *Laurencia luzonensis*. J Nat Prod 64:696–700

Kuniyoshi M, Wahome PG, Miono T, Hashimoto T, Yokoyama M, Shrestha KL, Higa T (2005) Terpenoids from *Laurencia luzonensis*. J Nat Prod 68:1314–1317

Lee HS (2006) Antiplatelet property of *Curcuma longa* L. rhizome-derived ar-turmerone. Bioresour Technol 97:1372–1376

Lee E, Surh Y-J (1998) Induction of apoptosis in HL-60 cells by pungent vanilloids, [6]-gingerol and [6]-paradol. Cancer Lett 134:163–168

Lee HS, Seo EY, Kang NE, Kim WK (2008) [6]-Gingerol inhibits metastasis of MDA-MB-231 human breast cancer cells. J Nutr Biochem 19:313–319

Li M-M, Jiang Z-E, Song L-Y, Quan Z-S, Yu H-L (2017) Antidepressant and anxiolytic-like behavioral effects of erucamide, a bioactive fatty acid amide, involving the hypothalamus-pituitary-adrenal axis in mice. Neurosci Lett 640:6–12

Liao J-C, Tsai J-C, Liu C-Y, Huang H-C, Wu L-Y, Peng W-H (2013) Antidepressant-like activity of turmerone in behavioral despair tests in mice. BMC Complement Altern Med 13:299

Liu M, Hansen PE, Lin X (2011) Bromophenols in marine algae and their bioactivities. Mar Drugs 9:1273–1292

Lu Z-H, Mu Y-M, Wang B-A, Li X-L, Lu J-M, Li J-Y, Pan C-Y, Yanase T, Nawata H (2003) Saturated free fatty acids, palmitic acid and stearic acid, induce apoptosis by stimulation of ceramide generation in rat testicular Leydig cell. Biochem Biophys Res Commun 303:1002–1007

Maran VBA, Josmeh D, Tan JK, Yong YS, Shah MD (2021) Efficacy of the aqueous extract of *Azadirachta indica* against the marine parasitic leech and its phytochemical profiling. Molecules 26:1908

Marques CNH, Davies DG, Sauer K (2015) Control of biofilms with the fatty acid signaling molecule cis-2-decenoic acid. Pharmaceuticals 8:816–835

Masuda M, Takahashi Y, Okamoto K, Matsuo Y, Suzuki M (1997) Morphology and halogenated secondary metabolites of *Laurencia snackeyi* (Weber-van Bosse) stat. nov. (Ceramiales, Rhodophyta). Eur J Phycol 32:293–301

Meden A, Knez D, Jukic M, Brazzolotto X, Grsic M, Pislar A, Zahirovic A, Kos J, Nachon F, Svete J, Gobec US (2019) Groselj: tryptophan-derived butyrylcholinesterase inhibitors as promising leads against Alzheimer's disease. Chem Commun 55:3765–3768

Mendez D, Gaulton A, Bento AP, Chambers J, De Veij M, Félix E, Magariños MP, Mosquera JF, Mutowo P, Nowotka M, Gordillo-Marañón M (2019) ChEMBL: towards direct deposition of bioassay data. Nucleic Acids Res 47:930–940

Moraes MCB, Birkett MA, Gordon-Weeks R, Smart LE, Martin JL, Pye BJ, Bromilow R, Pickett JA (2008) cis-Jasmone induces accumulation of defence compounds in wheat, *Triticum aestivum*. Phytochemistry 69:9–17

Murphy RC (2015) Tandem mass spectrometry of lipids: Molecular analysis of complex lipids. R Soc Chem

Nachon F, Carletti E, Ronco C, Trovaslet M, Nicolet Y, Jean L, Renard PY (2013) Crystal structures of human cholinesterases in complex with huprine W and tacrine: elements of specificity for anti-Alzheimer's drugs targeting acetyl- and butyryl-cholinesterase. J Biochem J 453:393–399

Niemoller TD, Bazan NG (2010) Docosahexaenoic acid neurolipidomics. Prostaglandins Other Lipid Mediat 91:85–89

Obici S, Feng Z, Morgan K, Stein D, Karkanias G, Rossetti L (2002) Central administration of oleic acid inhibits glucose production and food intake. Diabetes 51:271–275

Ohishi K, Toume K, Arai MA, Sadhu SK, Ahmed F, Ishibashi M (2015) Coronaridine, an iboga type alkaloid from *Tabernaemontana divaricata*, inhibits the Wnt signaling pathway by decreasing β-catenin mRNA expression. Bioorg Med Chem Lett 25:3937–3940

Palaniveloo K, Vairappan CS (2014) Chemical relationship between red algae genus Laurencia and sea hare (*Aplysia dactylomela* Rang) in the North Borneo Island. J Appl Phycol 26:1199–1205

Palaniveloo K, Rizman-Idid M, Nagappan T, Abdul Razak S (2020) Halogenated metabolites from the diet of *Aplysia dactylomela* Rang. Molecules 25:815

Palomer X, Pizarro-Delgado J, Barroso E, Vázquez-Carrera M (2018) Palmitic and oleic acid: the Yin and Yang of fatty acids in type 2 diabetes mellitus. Trends Endocrinol Metab 29:178–190

Park SY, Jin ML, Kim YH, Kim Y, Lee SJ (2012) Anti-inflammatory effects of aromatic-turmerone through blocking of NF-κB, JNK, and p38 MAPK signaling pathways in amyloid β-stimulated microglia. Int Immunopharmacol 14:13–20

Pechère M, Germanier L, Siegenthaler G, Pechère JC, Saurat JH (2002) The antibacterial activity of topical retinoids: the case of retinaldehyde. Dermatology 205:153–158

Pinzi L, Rastelli G (2019) Molecular docking: shifting paradigms in drug discovery. Int J Mol Sci 20:4331

Salem N Jr, Litman B, Kim H-Y, Gawrisch K (2001) Mechanisms of action of docosahexaenoic acid in the nervous system. Lipids 39:945–959

Srivastava P, Tripathi PN, Sharma P, Rai SN, Singh SP, Srivastava RK, Shankar S, Shrivastava SK (2019) Design and development of some phenyl benzoxazole derivatives as a potent acetylcholinesterase inhibitor with antioxidant property to enhance learning and memory. Eur J Med Chem 163:116–135

Stuhlmeier KM, Tarn C, Bach FH (1997) The effect of 5,8,11,14-eicosatetraynoic acid on endothelial cell gene expression. Eur J Pharmacol 325:209–219

Sud M, Fahy E, Cotter D, Brown A, Dennis EA, Glass CK, Merrill AH, Murphy RC Jr, Raetz CRH, Russell DW, Subramaniam S (2006) Lmsd: lipid maps structure database. Nucleic Acids Res 35:527–532

Suzuki M, Vairappan CS (2005) Halogenated secondary metabolites from Japanese species of the red algal genus *Laurencia* (Rhodomelaceae, Ceramiales). Curr Top Phytochem 7:1–34

Tan KL, Matsunaga S, Vairappan CS (2011) Halogenated chamigranes of red alga *Laurencia snackeyi* (Weber-van Bosse) Masuda from Sulu-Sulawesi Sea. Biochem Syst Ecol 39:213–215

Tripathi PN, Srivastava P, Sharma P, Tripathi MK, Seth A, Tripathi A, Rai SN, Singh SP, Shrivastava SK (2019) Biphenyl-3-oxo-1, 2, 4-triazine linked piperazine derivatives as potential cholinesterase inhibitors with anti-oxidant property to improve the learning and memory. Bioorg Chem 85:82–96

Vairappan CS, Tan KL (2005) Halogenated secondary metabolites from sea hare *Aplysia dactylomela*. Malays J Sci 24:17–22

Vairappan CS, Kawamoto T, Miwa H, Suzuki M (2004) Potent antibacterial activity of halogenated compounds against antibiotic-resistant bacteria. Planta Med 70:1087–1090

Vairappan CS, Anangdan SP, Tan KL (2007) Additional halogenated secondary metabolites from the sea hare *Aplysia dactylomela*. Malays J Sci 26:57–64

Vairappan CS, Anangdan SP, Matsunaga S (2009) Diet-derived halogenated metabolite from the sea hare *Aplysia parvula*. Malays J Sci 28:269–273

Vairappan CS, Kamada T, Lee WW, Jeon YJ (2013) Anti-inflammatory activity of halogenated secondary metabolites of *Laurencia snackeyi* (Weber-van Bosse) Masuda in LPS-stimulated RAW 264.7 macrophages. J Appl Phycol 25:1805–1813

Viayna E, Coquelle N, Cieslikiewicz-Bouet M, Cisternas P, Oliva CA, Sanchez-Lopez E, Ettcheto M, Bartolini M, De Simone A, Ricchini M, Rendina M (2020) Discovery of a potent dual inhibitor of acetylcholinesterase and butyrylcholinesterase with antioxidant activity that alleviates Alzheimer-like pathology in old APP/PS1 mice. J Med Chem 64:812–839

Wanke T, Philippus AC, Zatelli GA, Vieira LFO, Lhullier C, Falkenberg M (2015) C_{15} acetogenins from the Laurencia complex: 50 years of research-an overview. Rev Bras 25:569–587

Wei C-K, Tsai Y-H, Korinek M, Hung P-H, El-Shazly M, Cheng Y-B, Wu Y-C, Hsieh T-J, Chang F-R (2017) 6-Paradol and 6-shogaol,

the pungent compounds of ginger, promote glucose utilization in adipocytes and myotubes, and 6-paradol reduces blood glucose in high-fat diet-fed mice. Int J Mol Sci 18:16

Wijesinghe WAJP, Kang MC, Lee WW, Lee HS, Kamada T, Vairappan CS, Jeon YJ (2014) 5β-hydroxypalisadin b isolated from red alga *Laurencia snackeyi* attenuates inflammatory response in lipopolysaccharide-stimulated raw 264.7 macrophages. Algae 29:333–341

Xie Y, Peng Q, Ji Y, Xie A, Yang L, Mu S, Li Z, He T, Xiao Y, Zhao J (2021) Isolation and identification of antibacterial bioactive compounds from *Bacillus megaterium* L2. Front Microbiol 12:645484

Xu X, Huang M, Zou X (2018) Docking-based inverse virtual screening: methods, applications, and challenges. Biophys Rep 4:1–16

Young H-Y, Luo Y-L, Cheng H-Y, Hsieh W-C, Liao J-C, Peng W-H (2005) Analgesic and anti-inflammatory activities of [6]-gingerol. J Ethnopharmacol 96:207–210

Yue GG-L, Kwok H-F, Lee JK-M, Jiang L, Chan K-M, Cheng L, Wong EC-W, Leung P-C, Fung K-P, Lau CB-S (2015) Novel anti-angiogenic effects of aromatic-turmerone, essential oil isolated from spice turmeric. J Funct Foods 15:243–253

Zhan G, Gao B, Zhou J, Liu T, Zheng G, Jin Z, Yao G (2023) Structurally diverse alkaloids with nine frameworks from *Zephyranthes candida* and their acetylcholinesterase inhibitory and anti-inflammatory activities. Phytochemistry 207:113564

Zhu S, Jiao W, Xu Y, Hou L, Li H, Shao J, Zhang X, Wang R, Kong D (2021) Palmitic acid inhibits prostate cancer cell proliferation and metastasis by suppressing the PI3K/Akt pathway. Life Sci 286:120046

Ziouzenkova O, Orasanu G, Sharlach M, Akiyama TE, Berger JP, Viereck J, Hamilton JA, Tang G, Dolnikowski GG, Vogel S, Duester G, Plutzky J (2007) Retinaldehyde represses adipogenesis and diet-induced obesity. Nat Med 13:695–702

Springer Nature or its licensor (e.g. a society or other partner) holds exclusive rights to this article under a publishing agreement with the author(s) or other rightsholder(s); author self-archiving of the accepted manuscript version of this article is solely governed by the terms of such publishing agreement and applicable law.

Authors and Affiliations

Kishneth Palaniveloo[1,2] · Kuan Hung Ong[1] · Herland Satriawan[1] · Shariza Abdul Razak[3] · Suciati Suciati[4] · Hsin-Yi Hung[5] · Shin Hirayama[6] · Mohammed Rizman-Idid[1] · Jen Kit Tan[7] · Yoong Soon Yong[8] · Siew-Moi Phang[1,8]

✉ Kishneth Palaniveloo
kishneth@um.edu.my

Kuan Hung Ong
vandrossokh@gmail.com

Herland Satriawan
herlandsatriawan11@gmail.com

Shariza Abdul Razak
shariza@usm.my

Suciati Suciati
suciati@ff.unair.ac.id

Hsin-Yi Hung
z10308005@ncku.edu.tw

Shin Hirayama
st9828@cc.saga-u.ac.jp

Mohammed Rizman-Idid
rizman@um.edu.my

Jen Kit Tan
jenkittan@ukm.edu.my

Yoong Soon Yong
yongys.beach@gmail.com

Siew-Moi Phang
phang@um.edu.my

1 Institute of Ocean and Earth Sciences, Advanced Studies Complex, Universiti Malaya, 50603 Wilayah Persekutuan Kuala Lumpur, Malaysia

2 Centre for Natural Products Research and Drug Discovery (CENAR), Level 3, Research Management & Innovation Complex, Universiti Malaya, 50603 Wilayah Persekutuan Kuala Lumpur, Malaysia

3 School of Health Sciences, Nutrition and Dietetics Program, Health Campus, Universiti Sains Malaysia, 16150 Kubang Kerian, Kelantan, Malaysia

4 Department of Pharmaceutical Sciences, Campus C-UNAIR, Faculty of Pharmacy, Universitas Airlangga, East Java, Surabaya 60115, Indonesia

5 School of Pharmacy, College of Medicine, National Cheng Kung University, 70101 Tainan, Taiwan

6 Regional Innovation Center, Saga University, 1, Honjo, Saga 840-8502, Japan

7 Department of Biochemistry, Faculty of Medicine, Universiti Kebangsaan Malaysia, Jalan Yaacob Latif, Bandar Tun Razak, 56000 Wilayah Persekutuan Kuala Lumpur, Malaysia

8 Faculty of Applied Sciences, UCSI University, 56000 Wilayah Persekutuan Kuala Lumpur, Malaysia